

Miniature Neurologgers for Flying Pigeons: Multichannel EEG and Action and Field Potentials in Combination With GPS Recording

Alexei L. Vyssotski, Andrei N. Serkov, Pavel M. Itskov, Giacomo Dell'Omo,
Alexander V. Latanov, David P. Wolfer and Hans-Peter Lipp

JN 95:1263-1273, 2006. First published Oct 19, 2005; doi:10.1152/jn.00879.2005

You might find this additional information useful...

This article cites 25 articles, 2 of which you can access free at:

<http://jn.physiology.org/cgi/content/full/95/2/1263#BIBL>

Updated information and services including high-resolution figures, can be found at:

<http://jn.physiology.org/cgi/content/full/95/2/1263>

Additional material and information about *Journal of Neurophysiology* can be found at:

<http://www.the-aps.org/publications/jn>

This information is current as of February 1, 2006 .

Miniature Neurologgers for Flying Pigeons: Multichannel EEG and Action and Field Potentials in Combination With GPS Recording

Alexei L. Vyssotski,¹ Andrei N. Serkov,² Pavel M. Itskov,³ Giacomo Dell’Omo,¹
Alexander V. Latanov,^{1,2} David P. Wolfer,¹ and Hans-Peter Lipp¹

¹Institute of Anatomy, Division of Neuroanatomy and Behavior, University of Zürich, Zurich, Switzerland;

²Chair of Higher Nervous System Activity, Faculty of Biology, Moscow State University and

³P. K. Anokhin’s Institute of Normal Physiology, Department of Systemogenesis, Moscow, Russia

Submitted 19 August 2005; accepted in final form 16 October 2005

Vyssotski, Alexei L., Andrei N. Serkov, Pavel M. Itskov, Giacomo Dell’Omo, Alexander V. Latanov, David P. Wolfer, and Hans-Peter Lipp. Miniature neurologgers for flying pigeons: multichannel EEG and action and field potentials in combination with GPS recording. *J Neurophysiol* 95: 1263–1273, 2006. First published October 19, 2005; doi:10.1152/jn.00879.2005. To study the neurophysiology of large-scale spatial cognition, we analyzed the neuronal activity of navigating homing pigeons. This is not possible using conventional radio-telemetry suitable for short distances only. Therefore we developed a miniaturized data logger (“neurologger”) that can be carried by a homing pigeon on its back, in conjunction with a micro-global position system (GPS) logger recording the spatial position of the bird. In its present state, the neurologger permits recording from up to eight single-ended or differential electrodes in a walking or flying pigeon. Inputs from eight independent channels are preamplified, band-pass filtered, and directed to an eight-channel, 10-bit analog-digital converter of the microcontroller storing data on a “Multimedia” or “Secure Digital” card. For electroencephalography (EEG), the logger permits simultaneous recordings of up to eight channels during maximally 47 h, depending on memory, while single unit activity from two channels can be stored over 9 h. The logger permits single unit separation from recorded multiunit signals. The neurologger with GPS represents a better alternative to telemetry that will eventually permit to record neuronal activity during cognitive and innate behavior of many species moving freely in their habitats but will also permit automated high-throughput screening of EEG in the laboratory.

INTRODUCTION

The homing pigeon is an uniquely suited species for studying the neurophysiology of large-scale spatial cognition (Bingman et al. 2005). This would necessarily require the recording of brain activity during navigation. The commonly used radio-telemetry is unsuitable for this purpose, despite of the many miniaturized solutions developed already 30 years ago (Kimnich and Vos 1972; Mackay 1968). Meanwhile, several elegant solutions were developed for telemetrical multichannel EEG recording (Perkins 1980; Suess and Goiser 1986; Wertz et al. 1976; Yonezawa et al. 1979) as well as for single-unit recording (see e.g., Grohrock et al. 1997; Hawley et al. 2002; Nieder 2000; Obeid et al. 2004a,b; Pinkwart and Borchers 1987; Takeuchi and Shimoyama 2004; Winter 1998 to name a few). Several manufacturers also offer radio-telemetry now. However, recording from navigating homing pigeons would

require powerful senders and heavy batteries radio-transmitting high-quality signals over many kilometers. A bird weighing 400–500 g cannot carry such packages. The use of standard radio-telemetry on a flying pigeon might be possible only by following it with a helicopter, causing extremely high-costing experiments.

Another approach is data logging, for example as employed using magnetic tape (Ebersole 1987) and nowadays with flash memory. However, even the latter devices, chiefly used for patient monitoring in hospitals (Horikawa and Harada 1997), are unsuitable for placing them on small animals, particularly on flying pigeons, because they weigh >300 g (Siesta, www.compumedics.com).

Here we describe a newly developed miniature multichannel EEG and action and field potential data logger (“Neurologger”) that records and stores EEG simultaneously from eight electrodes or from eight differential pairs of electrodes. This device was used successfully to record brain activity of flying pigeons and may also be applied in a variety of other investigations with common laboratory animals. Action and field potentials can be recorded from two electrodes simultaneously in its present state, but the number of channels can be increased without much gain in weight by sandwiching several of these devices.

METHODS

Construction of data logger

A complete view of the logger and of its placement on a pigeon is given in Fig. 1. Schematics of the analog and digital parts are presented in Figs. 2 and 3, respectively. Complete schematics, circuit boards Gerber files, a complete bill of material, binary codes of microcontroller program, and PC interface utility may be found at <http://www.vyssotski.ch/neurologger>. The construction of the GPS data logger was described previously in Steiner et al. (2000); novel data sheets are available at <http://www.newbehavior.com>.

INPUT RANGES. To have optimal quality of digitization, different input ranges were chosen for recording of signals of different nature. EEG (bandwidth: 1–115 Hz) input range was $\pm 750 \mu\text{V}$, action potentials (bandwidth: 300–3,000 Hz) input range was $\pm 500 \mu\text{V}$, and wide-band recording (EEG + neuronal activity, 1–3000 Hz) was $\pm 1 \text{ mV}$.

AMPLIFICATION. The required amplification coefficient was split up into three amplification stages. The first stage amplifiers (Headstage

Address for reprint requests and other correspondence: A. L. Vyssotski, Institute of Anatomy, University of Zürich, Winterthurerstrasse 190, CH-8057 Zürich, Switzerland (E-mail: visotsky@anatom.unizh.ch).

The costs of publication of this article were defrayed in part by the payment of page charges. The article must therefore be hereby marked “advertisement” in accordance with 18 U.S.C. Section 1734 solely to indicate this fact.

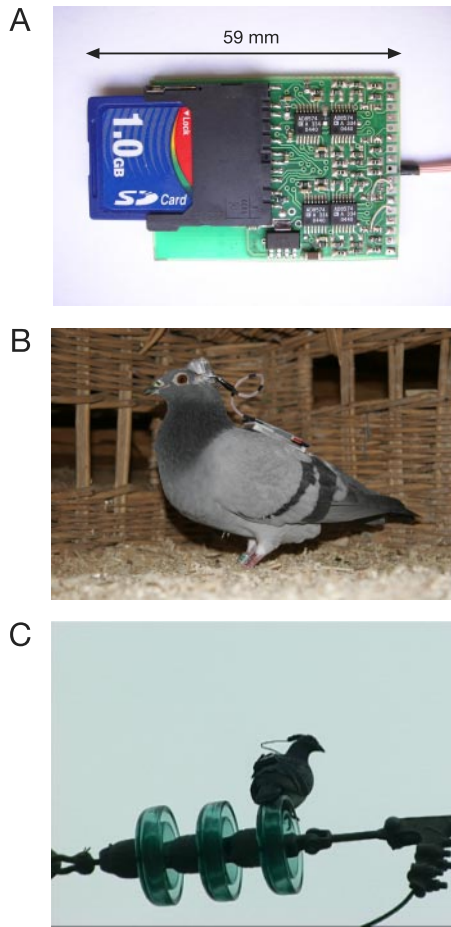


FIG. 1. Neurologger and its use on pigeons. *A*: 8-channel electroencephalographic (EEG)/single-unit data logger with 1 GB of storage capacity. *B*: neurologger for single unit recording attached to the back of a pigeon. The preamplifier is integrated into the connectors of the microdrive assembly on the head of the pigeon (covered with adhesive tape). *C*: pigeon carrying a combined EEG/global positioning system (GPS) logger on its back and resting on power line. On such (rare) occasions, electrical noise can be picked up by the logger otherwise largely insensitive to it.

amplifiers, labeled as amp 3 at Fig. 2*C*) were placed on a microboard directly connected to the head of a pigeon to diminish artifacts of the data transmission through the cables between the head and the data logger on the back of a pigeon. The amplification coefficient of the

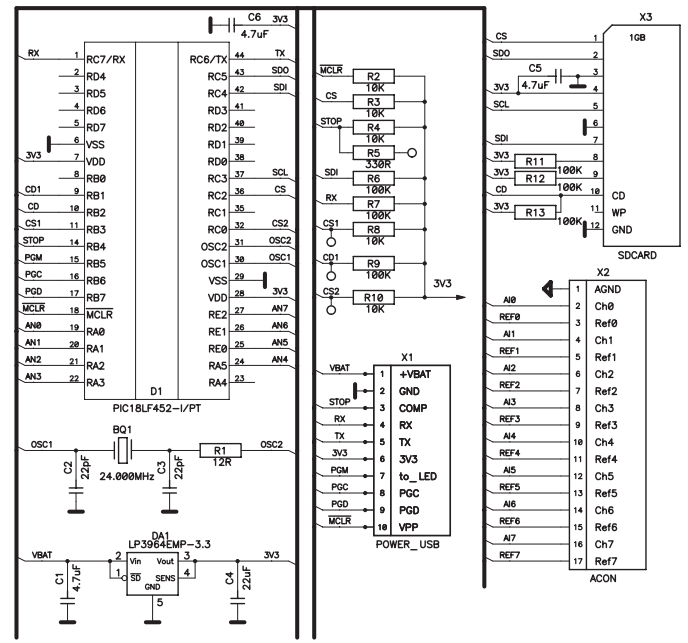


FIG. 3. Schematic for a digital part of the neurologger and a connector for analog signals X2. The main components of the digital part are microcontroller D1 and flash X3. The scheme also includes voltage regulator DA1, microcontroller quartz BQ1 and connector X1 for the data downloading and microcontroller reprogramming.

first cascade was 5.02. A unity gain source follower was used for the buffering of the signal from the reference electrode (Fig. 2*A*, amp 1). Amplifiers inputs were pulled to the headstage analog ground (AGND) by 120 M resistors to prevent polarization of electrodes by input currents of the amplifiers and to avoid pinning if inputs are disconnected. Low-noise low-voltage amplifiers AD8607/AD8609 (Analog Devices) were employed in all stages of the amplification cascade because of their small power consumption (40 μ A per amplifier). However, other types also can be used (for example, AD8574, pictured in Fig. 1*A*). After the first stage with no filtration at all, signals went through the differential amplifier (2nd stage, amp 4 at Fig. 2*C*) with a unit gain to subtract the reference potential from them. This was done to keep common mode rejection ratio (CMRR) of the differential cascade as low as 100 in the whole frequency range of the device. Afterward, the differential amplifier in the 1- to 3,000- and 300- to 3,000 Hz versions of device signals went through the first order passive low-pass filter ($F_{-3dB} = 3,000$ Hz) formed by resistor

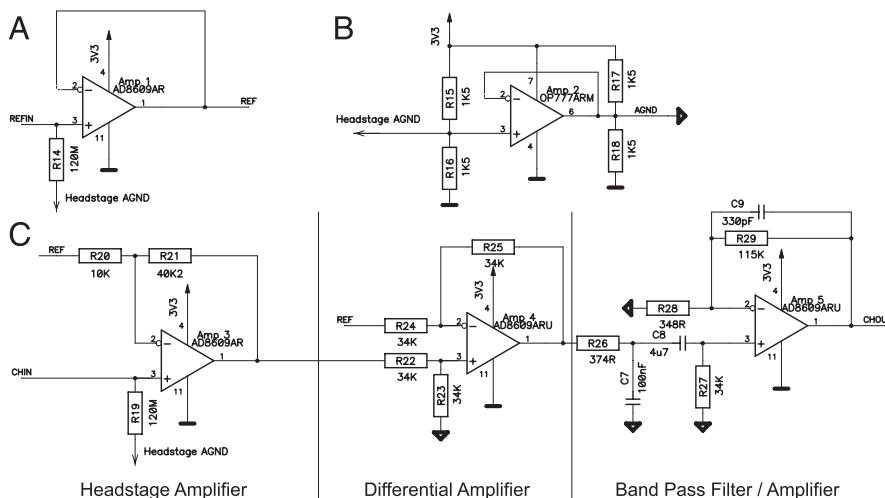


FIG. 2. Schematic for an analog part of the neurologger. *A*: unity gain amplifier of the reference electrode. *B*: analog ground-stabilizing circuitry. *C*: full analog front end channel (there are 8 identical channels in total). Inputs REFIN and CHIN are taken from the corresponding electrodes at the head of the animal. "headstage AGND" output connects to GND electrode at the animal head. CHOUT connects to the microcontroller ADC with a built in 8:1 multiplexer. Values at the scheme are for the wide-band (1–3,000 Hz) version of the device. Distinctions of other versions are described in the text.

R26 and capacitor C7. This passive filter was omitted in the low-frequency (1–300 Hz) device. After this stage, signals went through the first-order passive high-pass filter ($F_{-3dB} = 1$ or 300 Hz). Finally they were amplified by the third cascade with the appropriate gain to meet a 3.3 V input range of the ADC. This stage also served as first order low-pass filter ($F_{-3dB} = 115$ or 3,000 Hz). Values of resistors and capacitors at Fig. 2C are for the wide-band (1–3,000 Hz) version of the device. High-frequency (300–3,000 Hz) version differs in values of R27 = 5K36, R28 = 174R and C8 = 100 nF. Low-frequency (1–115 Hz) version differs from the wide-band version in values R28 = 2K55, R29 = 510K and C9 = 2.7 nF.

POWER SUPPLY. The system was powered through a LP3964 (National Semiconductor) low drop-out 3.3-V voltage regulator (DA1 at Fig. 3) drawing from a 4.2-V 560 mAh polymeric battery serving also the GPS logger. The neurologger was sandwiched between GPS receiver and the flat polymeric battery (Fig. 1C). Analog ground potential (+1.65 V from the digital ground) was formed by a resistor-based divider R16, R15 and buffered with a unity gain source follower (analog devices OP777ARM, Amp 2 at Fig. 2B). The stability of AGND was improved by resistors R16, R17. However, because of a very high gain of the amplification, even small noise at the AGND produced by filters could degrade the stability of the circuitry. To avoid such self-excitation, the AGND potential for the headstage amplifier was driven directly from R16, R15 divider.

DATA RECORDING. Signals were digitized by a 10-bit ADC of PIC18LF452 microcontroller (Microchip, D1 at Fig. 3) running at 24 MHz (giving a formal performance of 6 million instructions per second (MIPS)). The microcontroller was programmed to write data onto a 1 GB Secure Digital card (SanDisk, X3 at Fig. 3) continuously. For short-lasting experiments, 64 or 128 MB Multimedia cards (SanDisk) were used instead. The physical and electronic specifications of the neurologger are summarized in Table 1. The PIC18LF452 microcontroller was programmed in C language (www.ccsinfo.com). The interface program for the PC handling data exchange and device configuration was written in Delphi 7.0 (www.borland.com). A fast USB to serial converter DPL-USB232M (www.dipdesign.com) was used for the data exchange with PC at a speed of 1.5 Mbps. CRC

TABLE 1. *Technical data*

Parameter	Value
EEG logger mechanical dimensions	59×36×4 mm ³
Total mechanical dimensions (EEG logger, GPS logger, battery)	66×36×18 mm ³
EEG logger weight without battery and headstage amplifier	7 g
Headstage amplifier weight (with cable)	2 g
Weight 560mAh battery	13 g
GPS logger weight	13 g
Total weight	35 g
Battery life time EEG logger, 8ch × 500sps; GPS logger, continuous mode 1 Hz	3 h 30 min
EEG logger, 8ch × 500sps	2 days 5 h
Single unit logger, 2ch × 10ksps	22 h 20 min
1GB SD card data filling time 8 channels, 500sps	1 day 23 h
2 channels, 10ksps	9 h 24 min
1GB data downloading time Through serial interface	2 h
Through MMC:SD reader	20 min
Interface 2 RS232 (3.3V level), 1.5Mbps, converted to USB via DLP-USB232M	
2 GPIO: for GPS synchronization and for Status LED, power supply	
Data format	Custom

calculation was used for data integrity verification during data downloading.

POSSIBLE IMPROVEMENTS OF THE ANALOG PART OF THE NEUROLOGGER. The earlier-described analog part works well, but it can be improved/simplified in several ways. First, 120M resistors pulling inputs to the AGND probably might be omitted. Second, adding only two resistors at the scheme Fig. 2A (10K between pins 1 and 2 of amp 1 instead of direct connection and 40K2 between pin 2 and “headstage AGND”) will form a 2-op amp instrumentation amplifier (Horovitz and Hill 1989) at the headstage, eliminating the necessity of differential cascade based on separate amp 4 on the main board. However, this will require buffering of the AGND of the headstage with an operational amplifier. Third, the low-pass R26, C7 filter may be omitted. Its combination with the R29, C9 filter forms the second order filter providing 40 dB per decade attenuation in the infinity. However, as it is equal to a combination of two passive RC filters, its attenuation near the cutoff frequency does not differ drastically from the cutoff of a simple first-order filter (charts and explanations can be found in Horovitz and Hill 1989). For making a sharper cutoff of the filter without increasing the number of operational amplifiers, one might realize a high pass Sallen-Key filter at amp 4 and a low-pass Sallen-Key filter at Amp 5 (similarly as it is done in Obeid et al. 2004a).

USE DURING EXPLORATION. The neurologger permits both simultaneous writing of data into the memory card and sending it to the PC via a fast 1.5 Mbps serial link. The last feature allows monitoring of recorded signals at the screen of the attached computer in real time. This feature is especially helpful while searching for neuronal activity when advancing a microelectrode. The on-line data received can also be saved on the PC for further analysis.

SYNCHRONIZATION OF THE NEUROLOGGER WITH GPS AND OTHER EXTERNAL DEVICES. For synchronization with the GPS, a simple start synchronization was achieved by means of a signal line coming from the neurologger to the GPS (which has additional input possibilities for external synchronization with other events). A precise synchronization of the record with external stimuli provided by other controlling devices could be desirable in many cases. Such synchronization can be achieved currently only by synchronization of the start of the record with an external clock linked with a stimulating equipment. The internal clock of the logger is quartz-stabilized with ±50-ppm frequency stability sufficient for most of applications. However, start synchronization might not be convenient or sufficient in some cases. The desired on-line synchronization can be done conveniently by arranging an infra-red (IR) link between the logger and external equipment. For example, by placing an IR phototransistor with a small supplementary circuitry at the logger and an IR emitter above the experimental arena. Synchronizing flashes of the IR emitter could be detected by the IR phototransistor and stored together with neuronal data in the logger. The possibility of such synchronization was taken into account during device development: the microcontroller of the logger has unused inputs routed at the PCB to the reserved pads and the structure of the stored data has reserved unused bits suitable for storing synchronization flags.

Animal handling and electrode implantation

Adult homing pigeons served as subjects for these experiments. All pigeons had been trained to return to their home loft from several remote release places. They were also habituated to carry a load on their back—using PVC dummies of the same weight and shape as the data logger assembly. The pigeons carried the dummy permanently. Dummy or logger assembly could be attached and removed to and from an adhesive Velcro strip attached to the back of the pigeon.

Varnish-covered nichrome electrodes ($d = 150 \mu\text{m}$) were used for intracranial EEG recording, and gold-covered watch screws for epidural EEG recording. Tetropdes were used for the action and field potentials recording. They were manufactured from $25 \mu\text{m}$ nichrome wire (A-M Systems) as described in Gray et al. (1995) and were mounted on a custom-made, manually operated, microdrive placed on the skull over the hippocampal formation. Pigeons were anesthetized with a combination of xylazine (1 mg/kg body wt im) and ketamine (5 mg/kg body wt im) and placed in a stereotaxic apparatus. The skin on the dorsal surface of the skull was opened along the midline, and the appropriate number of holes was drilled in the skull to expose the dura.

All electrodes were fixed to the skull with dental cement (Paladur, Heraeus Kulcer GmbH). Before implantation short elastic cables were soldered to all electrodes. After implantation of electrodes the free ends of these elastic cables were soldered to a flat 10-pin, 1.27 mm pitch male connector. This connector was fixed with dental cement at the head of the animal.

The configuration of electrode placements varied according to experiments. Placement was done according to stereotaxic coordinates as given by Karten and Hodos (1967), the anatomical terminology following the new nomenclature as proposed by Reiner et al. (2004). For EEG studies, electrodes were placed over the left and right hippocampus and hyperpallium apicale (formerly hyperstriatum accessorium). A pair of connected electrodes over the area corticoidea laterale (CDL) served as a reference electrode.

Just after implantation, impedance of all electrodes was measured. The impedance at 1 kHz was 50–200 k Ω for nichrome EEG electrodes and $\sim 5 \text{ k}\Omega$ for screw electrodes. Tips of tetrode electrodes were not gold-plated and their impedance ranged from 1.0 to 1.8 M Ω . Impedance of the ground electrode was measured with respect to a large electrode placed in the pigeon's beak temporarily. Each pigeon was given minimum of 3 days to recover after implantation. One day before the first flight, a short EEG record was done in the laboratory from each pigeon to test the electrode quality. The first flight after implantation was done with a dummy to check that pigeon had not lost motivation or homing ability after the operation. All operated pigeons homed without any problems. Operating and testing procedures have been approved by the local animal experimentation committees of the Veterinary Office of the Canton of Zurich, in compliance with Swiss, Italian, and Russian legislation, respectively.

RESULTS

Combining EEG and GPS recording on pigeons

The rationale of using EEG recordings during homing of pigeons equipped with GPS is to monitor attentional mechanisms during the flight. For example, it is reasonable to assume that pigeons perceive and use a landmark for navigation if their flight trajectory as assessed by GPS changes at a recognizable topographical point (Lipp et al. 2004). However, a pigeon might perceive many more navigationally relevant cues during the flight that may cause a change in direction, but it could also ignore such cues and maintain an unaltered course. Thus our primary goal was to record EEG activity expecting to identify the presence of cues that elicit the attention of the pigeon. In humans and mammals, perception of salient stimuli is often followed by desynchronization of slow wave electrical activity, e.g., Umbricht et al. (2004, 2005).

IDENTIFYING EVENT-RELATED SPECTRAL PERTURBATIONS. Before testing the neurologger during flight, we tested whether our assumption of EEG desynchronization on perception of sen-

sory stimuli would be valid for pigeons. After implantation with intracranial electrodes in various locations, pigeons were first tested in a sound-attenuated chamber and exposed to diverse auditory and visual stimuli. Every minute a 10-s sound or light was given, thus during 1-h session, a pigeon received 60 presentations. Different artificial and natural sounds (wings flops, pecking, sound of the door of the aviary, cooing) and also visual stimulation (constant light and blinking) were presented in a sequential order. Changes in the EEG spectrum produced by the stimulation during epochs of 60 s were then analyzed using the MATLAB environment (www.mathworks.com) with the help of EEGLAB package (Delorme and Makeig 2004).

A third-order regression polynomial was subtracted from each epoch to remove low-frequency channel floating. This practically eliminated the first harmonics from the Fourier spectrum, but this did not cause any problem in the further analysis because we were interested in high frequencies only ($>3 \text{ Hz}$). A further step was the subtraction of channels from each other to get the differential signal from two electrodes of interest. In this type of analysis, a pair of electrodes in the left hippocampus was used (Fig. 4B).

In most cases, sensory stimulation visibly diminished the EEG amplitude as seen in Fig. 4A. EEG reduction occurred synchronously in all channels located in different brain regions, however. This implies that the exact position of electrodes was not important for the analysis. The responses from three pigeons during 132 presentations with an epoch length of 60 s were then averaged and analyzed for event-related spectral perturbations (ERSP) according to Makeig (1993) and Delorme and Makeig (2004). The color-coded plots of these ERSP clearly signal systematic event-related shifts in the power spectrum (Fig. 4B). The most significant reduction of relative power induced by the stimulation occurred near a frequency of 7 Hz, i.e., in the theta frequency range, which is 3–7 Hz in pigeons (Siegel et al. 2000). The absolute EEG power in this theta frequency range is stronger than in the high-frequency ranges (alpha: 7–12 Hz; gamma: 12–30 Hz). Thus the power of the theta frequency range appeared to be a suitable measure of desynchronization caused by sensory stimulation.

EEG/GPS ANALYSIS DURING FLIGHT AND RESTING. Pigeons implanted with epidural electrodes were released from several locations between 1.1 and 22 km from the home loft. EEG (5–8 channels) was digitized with a sampling rate of 500 Hz, while the GPS logger stored positional data every second (Steiner et al. 2000) (www.newbehavior.com). Both data loggers were synchronized. After returning to the home loft, the devices were removed from the birds. A standard MMC/SD memory card reader read data from the SD memory card while data from the GPS logger were downloaded to the PC through a serial port.

For EEG data analysis, an epoch length of 1 s was chosen, according to the sampling rate of the GPS logger. For calculation of the EEG power during flight, two pairs of electrodes were used, one over the left hemisphere, over the left area corticoidea dorsolateralis (left CDL)—left hyperpallium apicale (left HA), the other pair over the right one (right CDL—right HA). Artifact-containing epochs were rejected by the

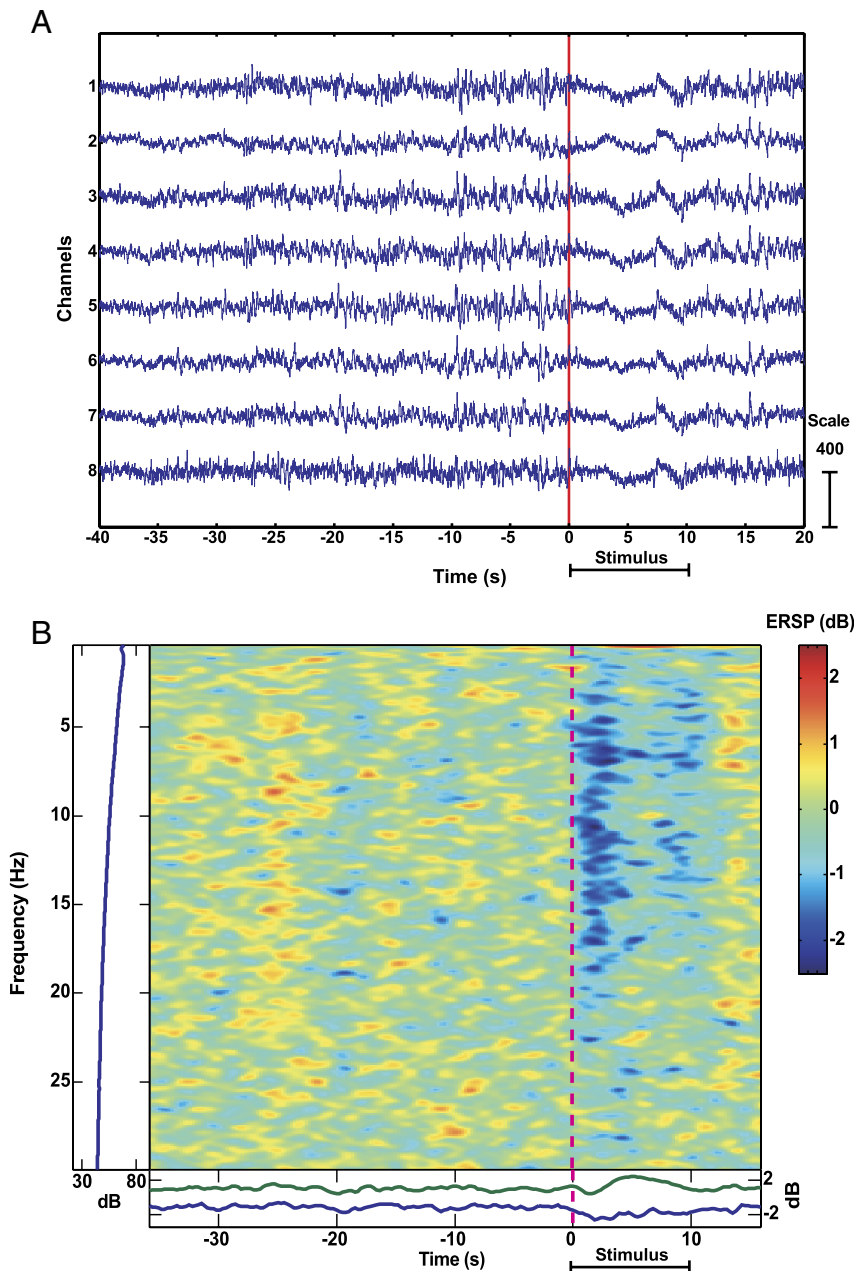


FIG. 4. Desynchronization of EEG in pigeons caused by stimulation. A vertical red line at *time 0* labels the start of the video/audio stimulation lasting for 10 s. *A*: original records of an epoch of 60 s. *B*: color-coded average of 132 presentations showing even-related spectral perturbations (ERSP), the strongest decrease in power indicated in blue and occurring strongly in the theta range (near 7 Hz). The vertical panel to the left shows the baseline mean power spectrum; the horizontal panel below the color-coding the ERSP envelope (low and high mean dB values, relative to baseline, at each time in the epoch).

methods included in the EEGLAB package: finding of abnormal values (threshold $\pm 200 \mu\text{V}$), finding improbable data (5 SD), finding abnormal distributions (5 SDs), and finding abnormal spectra ($\pm 30 \text{ dB}$ in range 0–50 Hz), according to Delorme et al. (2004). This procedure yielded an acceptable percentage of rejected data both in the flying (33.7%) and in the sitting (10.9%) pigeon.

Samples of EEG records obtained in a resting and flying pigeon are presented in Fig. 5. One may note the absence of any regular artifacts from rhythmic muscle activity in the flight, despite of the fact that the average speed of the pigeon in the flight was near 50 km/h. This allows analyzing such EEG records without any special preprocessing like principal component analysis (PCA) or independent component analysis (ICA). However, this is only the case when using low-impedance epidural electrodes. The intracranial wire electrodes are

much more sensitive to such disturbances and special preprocessing of data are needed to eliminate them.

As no hemispheric asymmetry was detected, the total power of the EEG was calculated as average of powers of the differential pairs (left CDL—left HA; right CDL—right HA) to diminish variability (Fig. 6). Additionally, charts were smoothed using a moving average filter with a span of 5 (Fig. 6A). This procedure clearly indicates that the EEG power in theta range (and also the total EEG power) was significantly diminished during the flight phases (Fig. 6A). This finding may indicate ongoing attentional processing in the brain of the pigeons due to sampling of familiar visual cues underlying spatial orientation in the vicinity of the home loft (Lipp et al. 2004). Figure 6B shows the color-coded power of the theta EEG range superimposed on the pigeon's trajectory as recorded by GPS. Evidently, power is not constant during the

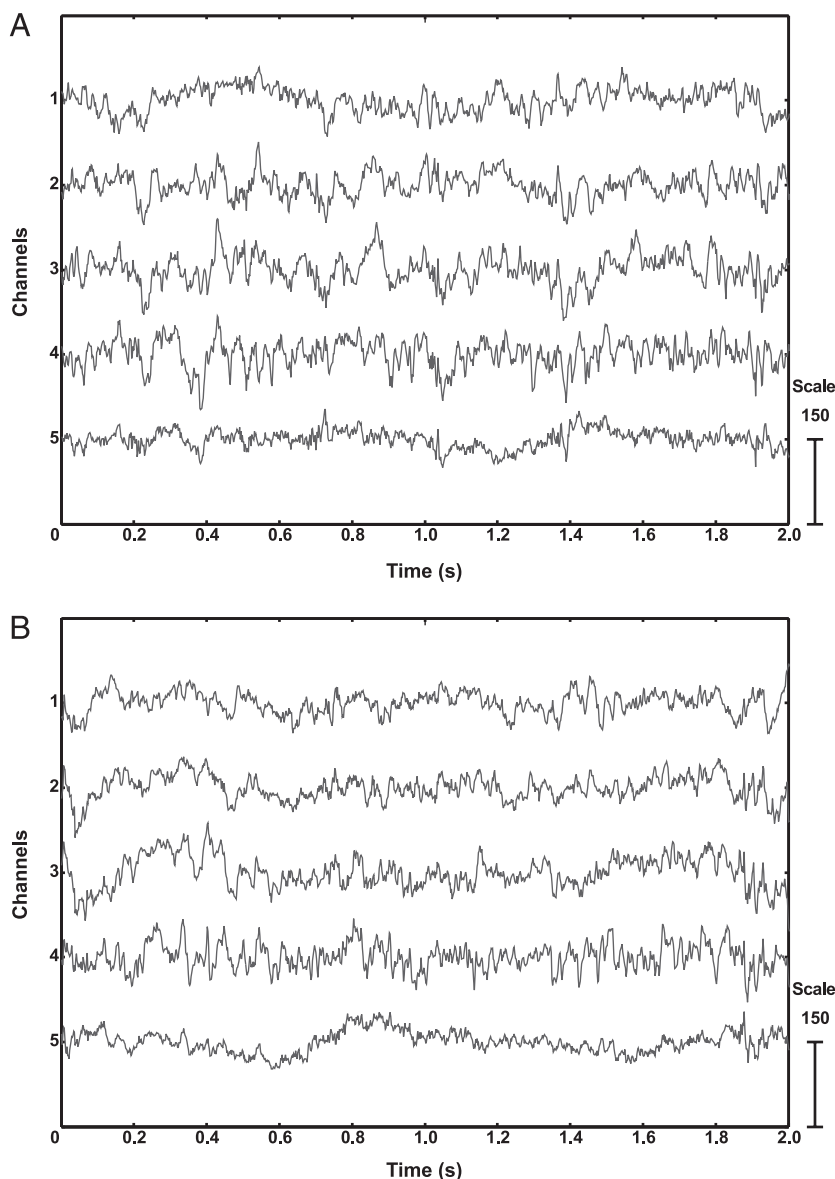


FIG. 5. EEG record from the flying (A) and resting pigeon (B) that are practically indistinguishable with respect to signal quality. Note in A the absence of any flight artifacts despite of a flight speed of ~ 50 km/h.

flight, but further data are needed to elucidate the physiological meaning of EEG power variations during pigeon flight and homing. Nonetheless, the combination of flight tracks on topographical maps and satellite pictures (Fig. 6C) with changing EEG data appears to be a highly promising approach. For example, the trajectory of the flight first follows a road (and not the home direction). Then the pigeon took a rest, after which it followed the road till an intersection where it corrected its course toward the loft reaching it across forests and meadows.

Recording action and field potentials during resting and flight

The final goal of our approach is to identify neuronal activity related to navigational behavior. This, however, can only be achieved if the neurologger has the same capacity in identifying and analyzing neuronal activity as found in conventional on-line systems.

EEG AND ACTION POTENTIAL RECORDING WITH A DISTANT REFERENCE ELECTRODE. Before experiments with a freely flying bird, single units were recorded using the neurologger in the anesthetized pigeon fixed in the stereotaxic apparatus in an acute experiment (Fig. 7A) and also from a chronically implanted tetrode in the awake pigeon sitting in the chamber (Fig. 7B). An epidural watch screw in the vicinity of the tetrode served as reference electrode during acute experiments, while an intracranial implanted nichrome wire of $150\ \mu\text{m}$ diam served as reference in the chronic experiment. A single-channel 16 ksp/s record was done to check the quality of the wide-band recording (1–3,000 Hz) by the system. A relatively good signal-to-noise ratio was observed in the acute experiment and several spikes from a selected neuron clearly indicate the ability of the neurologger to record single-unit activity. In the chronic implantation, the signal-to-noise ratio was less distinct, mainly because of the smaller spike amplitude, possibly related to the less controllable advancement of the miniature microdrive on the head of the pigeon. However, single

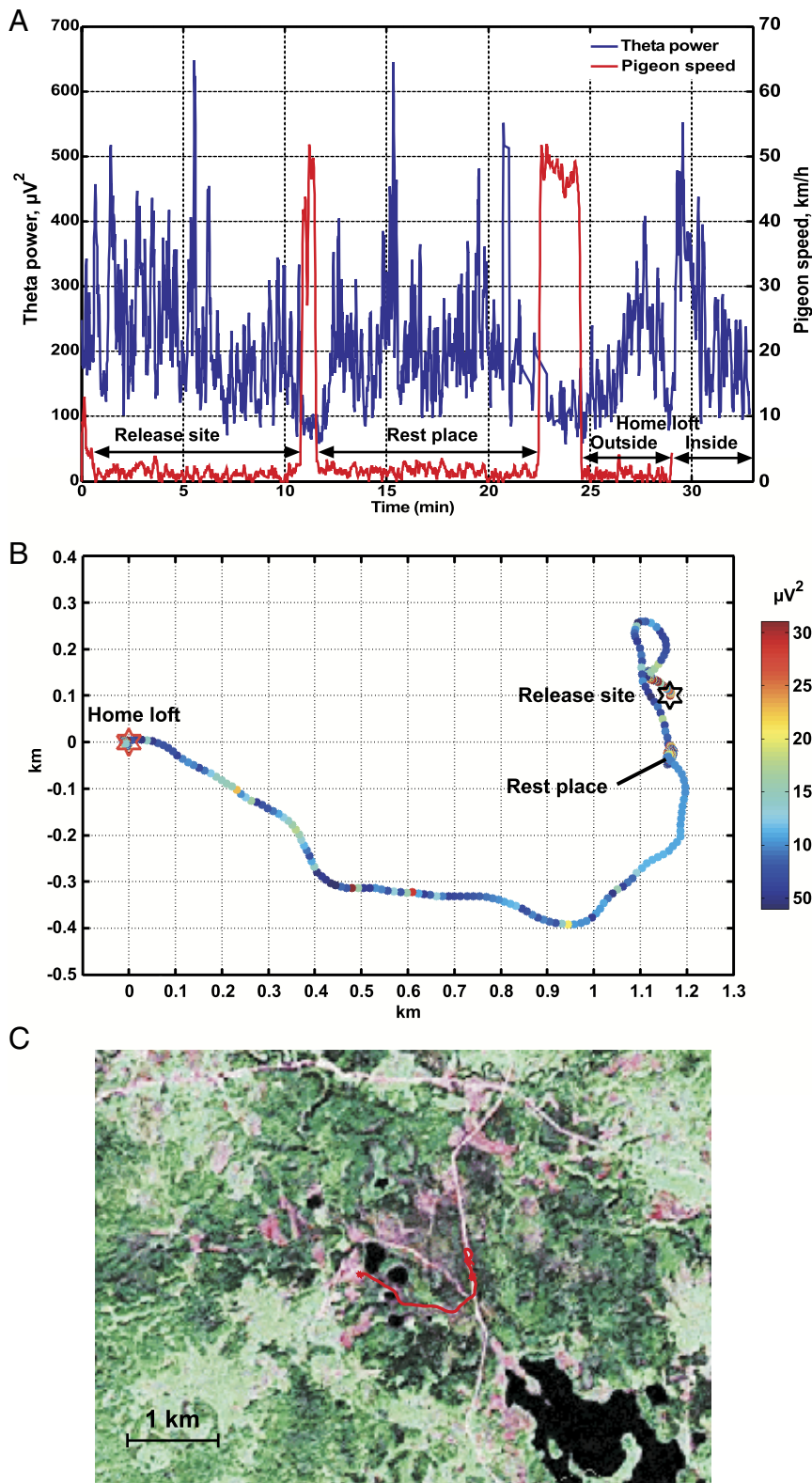


FIG. 6. Joint logging of EEG and GPS position data in a pigeon released over a short distance of ~ 1.2 km from the loft. *A*, in blue: theta power plots covering the time before release, during flight and a rest phase, and after arrival to the loft where the pigeon was first sitting on the top before moving in. Red: changes in speed as assessed by GPS recording. Note the strong decrease in power of theta range (3.5–7.0 Hz) during the 2 flight episodes and during flying from the roof to the loft entry. *B*: color-coded variations of theta power coded in epochs of 1 s (corresponding to ~ 12 –15 m when flying). Note the power reduction and the variations during flight that may indicate attentional processing of visual landmarks. *C*: superposition of GPS tracks on an infrared satellite image of the region (lakes: dark; roads: bright; forest: dark green; open vegetation: shades from reddish to yellow-green). Note that the pigeon first follows the road and not the home direction. After resting, it followed the road till a bifurcation pointing to the loft from where it took a shortcut across the meadows. This strongly implies the use of local landmarks.

spikes were still visible and could be separated from the wide-band EEG-single-unit record (Fig. 7*B*). The spectrum of the low-frequency activity did not differ much from the EEG spectrum as obtained with epidural electrodes (data not shown). Hence, the neurologger can be used to record simultaneously both EEG/field potentials and action potentials from tetrodes.

FIELD AND ACTION POTENTIAL RECORDING WITH IN-TETRODE REFERENCE. However, we have found that recordings with a distant reference electrode in a wakeful pigeon are highly sensitive to artifacts caused by locomotion, probably because of penetration of muscular electrical potentials into the brain from different places. In fact, these artifacts mostly exceeded

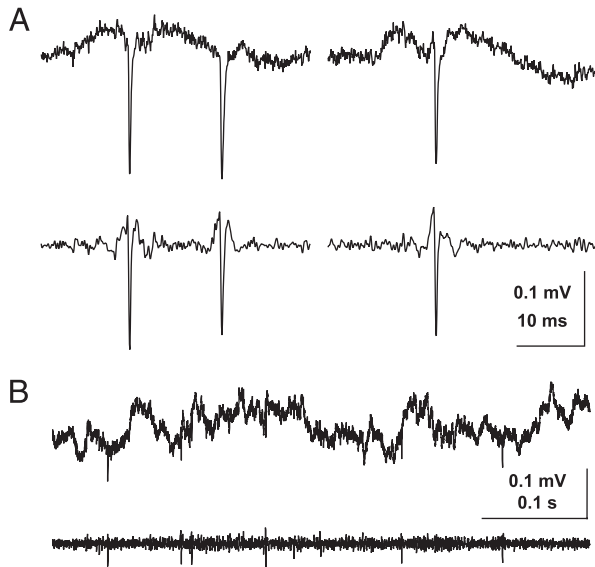


FIG. 7. Samples of neuronal wideband recordings and filtering obtained with the neurologger in an anesthetized pigeons (A) and after chronic implantation of electrodes while the pigeon was placed in a recording chamber but did not move (B). Only 1 channel of the tetrode was digitized with a rate of 16 kps; the external reference electrode was a low-impedance 150- μ m nichrome wire. Band-passed filtered recordings (300–3,000 Hz) are shown below the wide-band records in A and B, respectively. Note the ability of the logger to record EEG/local field potentials together with action potentials. The increased noise level (or reduced spike amplitude, respectively) in the chronic recording (B) probably reflects the poorer mechanical properties of the head-mounted mini-microdrive permitting less precise adjustments of electrode position as compared with the microdrive in the stereotaxic apparatus.

the input range of the device. If only action potentials are of interest, a high-pass filter may eliminate low-frequency artifacts due to locomotion, but recording wide-band activity needs another approach to dampen locomotion-induced artifacts during walking and particularly during flying. Thus we checked the possibility of using one channel of the tetrode as reference electrode for the remaining three electrode tips. This removes (long-distance) EEG potentials from the signal, but local field and action potentials will be recorded. On the other hand, the price paid for the reduction of movement artifacts is that using a high-impedance tetrode electrode as reference increases the total noise in the channels.

A sample of a 10-kHz two-channel record with an in-tetrode reference (Fig. 8A) shows one main difference to conventional extra-cellular recordings: spikes not only shoot down but also can shoot up when a cell is firing near the reference tip (marked with asterisks in Fig. 8A). The wing-flapping artifacts are still clearly visible but no longer exceed the input range of the neurologger (Fig. 9A), making the raw data amenable to various types of filtering.

SPIKE DETECTION. The continuously recorded wideband signals were digitally band-pass filtered (Hamming window-based finite impulse response filter, cutoffs at 300 and 3,000 Hz, filter order 250). The input data were processed both in forward and reverse directions. The resulting sequence had precisely zero-phase distortion and doubled the filter order. The average value of the filtered signal was computed in a sliding window (0.2 ms) for spike detection. Standard deviations were calculated to estimate the variance of the baseline noise and to establish detection thresholds. The estimation of the noise variance was

improved in the second iteration by including into calculation only nonoutlier time points (with a deviation <5 of the previously calculated SD). Spikes with the deviations A_i and B_i in channels A and B (at time point i) were extracted if $(A_i/\sigma_A)^2 + (B_i/\sigma_B)^2 > 25$ (σ_A and σ_B indicating SD of noise in the corresponding channels).

SPIKE SORTING. The extracted spike waveforms were separated on the basis of their spike amplitude and wave shape (Csicsvari et al. 1998). The spike waveforms were reconstructed to 40 kHz by using the principles of the sampling theorem (Press et al. 1992), and the peaks of the reconstructed waveforms were realigned. A time point i where the equation $(A_i/\sigma_A)^2 + (B_i/\sigma_B)^2$ reaches its maximum was taken as a center of the spike form. Instead of simple peak-to-peak measurement of the spike amplitude, all sampled amplitude values ± 1.35 ms from the peak were used to reduce noise-induced variance. Signals were down-sampled back to 10 kHz to reduce computational load. Thus each spike waveform consisted of 27 points. The information encoded in the amplitude values was com-

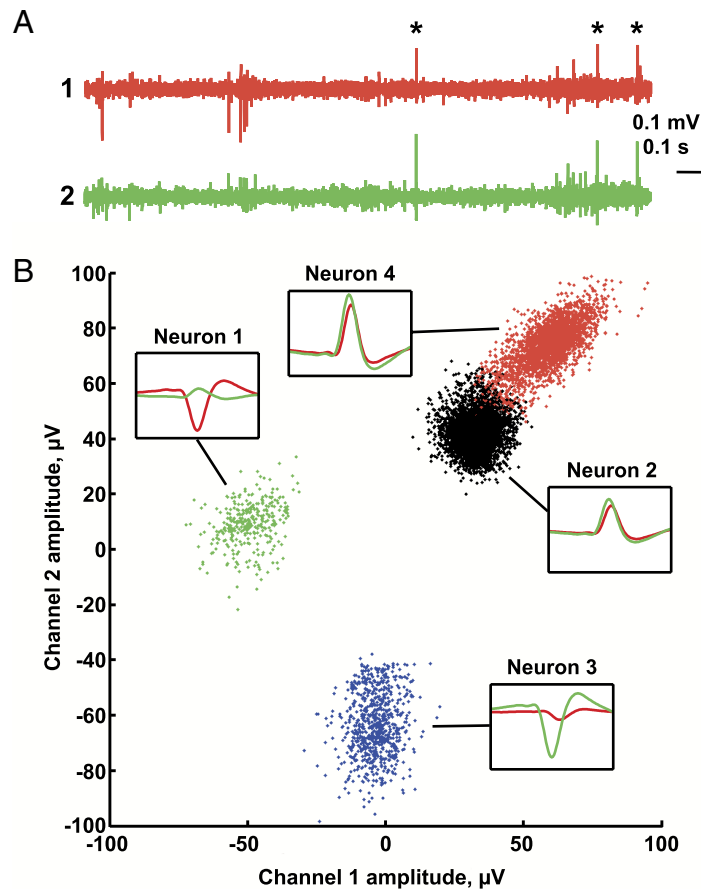


FIG. 8. Two-channel 10-kps recordings of action potentials using an in-tetrode reference. A: band-pass filtered activity patterns in the two channels. Note that neurons in the vicinity of the reference electrode give spikes directed upwards, clearly distinguishable from the activity near other electrode tips. This helps in separating neurons. B: cluster plots of spike activity in the 2 channels identifying 4 neurons and their average waveform during 2.7 ms. Amplitude range of the boxes is 120 μ V. Note good separation of the 4 units made by recording from 2 channels only. Neuron 1 appeared near the electrode tip 1 of the tetrode, neuron 3 near electrode 2, and cells 2 and 4 near the reference electrode. Neuron 1 is visible at the 1st half of the record sample at Fig. 8A, neuron 4 fires in the second half of this sample, its spikes indicated by asterisks.

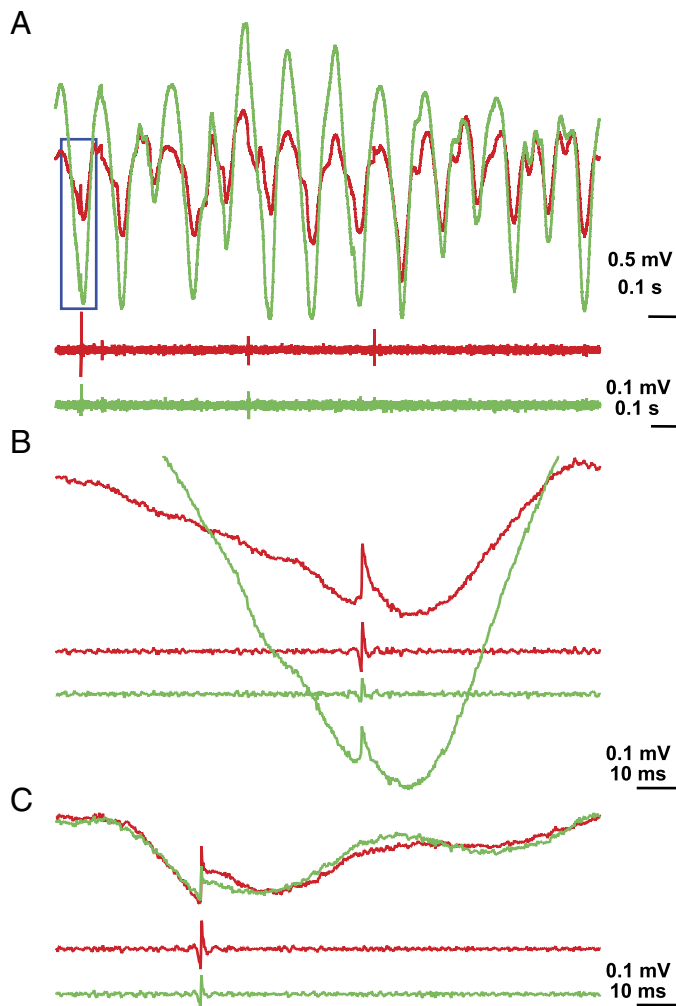


FIG. 9. Neuronal activity in a pigeon during flight and rest as recorded using an in-tetrode reference electrode implanted into the area parahippocampalis, coordinates AP 6.0, L 2.0, H 1.0; sampling rate 9 ksp/s. *A*: wideband extraction showing regular wing-flap artifacts with superimposed spikes in 2 channels (red and green). Below, the band-pass filtered (300–3,000 Hz) spike activity in the 2 channels. *B*: magnified part of the inset in *A* showing wideband and band-passed filtering of the 2 channels. *C*: activity of the same neuron during resting of the pigeon. Note the potential shift prior to spiking, characteristic for that neuron.

pressed using PCA. The first three principle components were calculated for each channel. Thus a single spike was represented by six waveform parameters as a six-dimensional feature vector. An automatic algorithm (“KlusterKwik”, available at <http://osiris.rutgers.edu/Buzsaki/software>), was used for isolating neurons, followed by manual clustering.

NEURONAL ACTIVITY IN RESTING PIGEON. The data from the logger clearly permit isolation of different neurons according to cluster plots and waveform (Fig. 8*B*). Neuronal activity at a tetrode placed in the Area parahippocampalis (stereotaxic coordinates AP6.0, L2.0, H1.0; 1 tetrode channel was used as reference) was recorded during 1 h in a resting pigeon. During recording, the pigeon was kept in a large cage separately from other birds. From the recordings, four cells were identified using information from two channels of the tetrode only. During this period the averaged firing rates of these four neurons were 0.092, 1.10, 0.21, and 0.73 spikes/s, respectively. These are low firing rates, even for pigeons (Siegel et al. 2005).

Thus temporal coincidence (overlapping) and annihilation of spikes at the reference and another electrode is unlikely. The noise-induced SDs were 5.37 and 5.76 μV for the first and the second channels, respectively. This level of noise is acceptable because the spike-detection thresholds (26.85 and 28.8 μV) calculated at the basis of these values do not cut clusters out of the detected neurons: these clusters have a decent oval shape (Fig. 8*B*). Possibly gold-plating of the electrode tips (Gray et al. 1995) might help to reduce noise in future experiments.

Our number of four separable units fits well with previously published results showing an average number of detected units of 1.8 for stereotrodes, and of 5.4 for tetrodes, respectively (Gray et al. 1995). The additional recording from the in-tetrode reference electrode obviously helps to identify single-unit activity without increasing the number of recording channels, limited to two at 10 ksp/s in the current logger version. This is especially valuable for miniature portable systems that have limited computational power and data storage but should have a wide input range permitting to record slow field potentials also.

NEURONAL ACTIVITY DURING FLIGHT. The data logger clearly permits to identify single-unit activity during both flight and resting using an in-tetrode reference for recording (Fig. 9). Two channel wide-band extraction revealed the rhythmic wing artifacts yet superimposed to them action potentials (Fig. 9*A*). Extracting the same signals with band-pass filtering (300–3,000 Hz) permitted to separate clearly the action potentials. A comparison of single spikes with high magnification, once from flight (Fig. 9*B*) and once from sitting just after landing outside (Fig. 9*C*), showed that the latter was preceded and followed by a slow potential drift. These potential drifts were typical for this neuron under sitting conditions, being associated with every spike, yet sometimes occurring without an action potential. While the significance of this neuronal behavior is unknown yet, it nicely illustrates the quality of the logger recordings.

DISCUSSION

The current article describes design and application of an eight-channel EEG- and two-channel action- and field-potential data logger that were used successfully to record EEG and neuronal activity in flying pigeons. The systems are capable to quantify and store eight analog channels simultaneously at EEG sampling rates and two channels at sampling rates needed for single-cell activity recording. They are characterized by small size, low weight, low power consumption, and absence of noise and channel crosstalk yet permitting high-quality data recording of EEG and action and field potentials. Thus they fully meet the demands for short- and long-term recordings in freely moving animals.

One of the main benefits of data logging in comparison with radio-telemetry is the possibility to use it under natural conditions where a big distance between animal and the experimenter makes radio-telemetry difficult because of size/power limitations. Up to now, we used EEG/neuronal recording in pigeons flying ≤ 22 km from the home loft. To link a pigeon with the home loft by radio at such distance is practically impossible given the small size of the bird. Moreover, accurate radio transmission depends much on topography and weather

conditions. Thus for such investigations data logging remains the only tool so far.

Another benefit of data logging is the quality of EEG neuronal activities recorded by multichannel registration. In traditional radio-telemetry of analog data, the transmitted voltage is not always fully proportional to the real voltage. In one-channel telemetry, the nonlinearity is usually not important, but when one subtracts two signals close to each other, as in case of multichannel EEG telemetry, the relative error can increase massively. Another problem intrinsic to multichannel radio-telemetry of analog signals is channel crosstalk. For such systems, it is assumed that a satisfactory crosstalk should be <2% (Perkins 1980). In our system, the nonlinearity and channels crosstalk are not detectable at all (<0.1% of the scale). Finally, multichannel telemetry systems with analog-digital conversion in the sender suffer from high power consumption, complexity, and weight. In addition to the transmission circuitry, they should have a microcontroller with ADC that also consumes significant amount of current.

Multichannel neurologgers can serve as an elegant tool to study brain-behavior interaction in freely behaving animals not only under naturalistic conditions. A final, not so obvious, advantage of our data logger is that it operates usually in environments without electrical noise typically present in laboratory installations without shielding.

On the other hand and given the high quality of multichannel recording, it could prove useful also in laboratory-based applications that do not require on-line supervision, for example epilepsy and sleep monitoring. For one, the costs are much lower than in conventional radio-telemetry. The production cost of the neurologgers fabricated in small amounts can be estimated as \$300. This sum splits into approximately equal parts between cost of 1GB flash, cost of other components, and cost of assembly work. The other point is that it allows the operation of many simultaneous recordings—something not easily achieved with radio-telemetry requiring different transmission frequencies or shielding of sender-receiver pairs. However, using the neurologger in the laboratory for interactive applications instead of radio-telemetric systems carries a minor inconvenience. The recorded signals are not visible to the experimenter in real time. This means that an on-line correction is not possible. This is an inherent feature of the neurologger that hardly can be compensated.

At present, the main disadvantage of the neurologger used is the necessity to link it with cables to the electrode socket on the head of the animal and its dependence of the battery carried on the back. However, having achieved satisfactory functionality with these prototypes, we are confident in our ability to miniaturize these loggers to the extent that they will fit entirely on the head of a small animal, including battery. This will allow the ultimate freedom for animal movement and neuronal recording in whatever environment.

ACKNOWLEDGMENTS

We appreciate the help, advice, and support from A. Loizzo at the Istituto Superiore di Sanità in Rome and thank I. Panova and A. Abramchuk with neurologgers development and manufacturing. We are particularly grateful to N. Bologova, S. Pazhetnova, N. Ben Abdallah, and C. and M. Calderoni for expert care of pigeons. We also thank two anonymous reviewers for helpful and constructive comments.

GRANTS

This work was supported by the Swiss National Foundation for Scientific Research, Scientific Co-operation between Eastern Europe and Switzerland 7IP62145, and the National Competence Center for Research Neural Plasticity and Repair.

REFERENCES

- Bingman VP, Gagliardo A, Hough II GE, Ioalé P, Kahn MC, and Siegel JJ. The avian hippocampus, homing in pigeons and the memory representation of large-scale space. *Integr Comp Biol* 45: 555–564, 2005.
- Chien C-N and Jaw F-S. Miniature telemetry system for the recording of action and field potentials. *J Neurosci Methods* 147: 68–73, 2005.
- Csicsvari J, Hirase H, Czurko A, and Buzsáki G. Reliability and state dependence of pyramidal cell-interneuron synapses in the hippocampus: an ensemble approach in the behaving rat. *Neuron* 21: 179–189, 1998.
- Delorme A and Makeig S. EEGLAB: an open source toolbox for analysis of single-trial EEG dynamics. *J Neurosci Methods* 134: 9–21, 2004.
- Ebersole JS. Ambulatory cassette EEG in epilepsy diagnosis. *Yale J Biol Med* 60: 85–91, 1987.
- Gray C, Maldonado P, Wilson M, and McNaughton B. Tetrodes markedly improve the reliability and yield of multiple single-unit isolation from multi-unit recordings in cat striate cortex. *J Neurosci Methods* 63: 43–54, 1995.
- Grohock P, Häusler U, and Jürgens U. Dual-channel telemetry system for recording vocalisation-correlated neuronal activity in freely moving squirrel monkeys. *J Neurosci Methods* 76: 7–13, 1997.
- Hawley E, Hargreaves E, Kubie J, Rivard B, and Muller R. Telemetry system for reliable recording of action potentials from freely moving rat. *Hippocampus* 12: 505–513, 2002.
- Horikawa M and Haragda H. Development of a portable multipurpose recorder using a 24-hour ambulatory recorder: application to polysomnography. *Med Biol Eng Comput* 35: 757–759, 1997.
- Horowitz P and Hill W. *The Art of Electronics*. Cambridge, UK: Cambridge Univ. Press, 1989.
- Karten HJ and Hodos W. *A Stereotaxic Atlas of the Brain of the Pigeon (Columba livia)*. Baltimore, MD: Johns Hopkins Press, 1967.
- Kimmich HP and Vos JA. *Biotelemetry*. Leiden: Meander, 1972.
- Lipp H-P, Vyssotski AL, Wolfer DP, Renaudineau S, Savini M, Tröster G, and Dell’Omo G. Pigeon homing along highways and exits. *Curr Biol* 14: 1239–1249, 2004.
- Mackay RS. *Bio-Medical Telemetry. Sensing and Transmitting Biological Information from Animals and Man*. New York: Wiley, 1968.
- Makeig S. Auditory event-related dynamics of the EEG spectrum and effects of exposure to tones. *Electroencephalogr Clin Neurophysiol* 86: 283–293, 1993.
- Nieder A. Miniature stereo radio transmitter for simultaneous recording of multiple single-neuron signals from behaving owls. *J Neurosci Methods* 101: 157–164, 2000.
- Obeid I, Nicolelis MAL, and Wolf PD. A low power multichannel analog front end for portable neural signal recordings. *J Neurosci Methods* 133: 27–32, 2004a.
- Obeid I, Nicolelis MAL, and Wolf PD. A multichannel telemetry system for single unit neural recordings. *J Neurosci Methods* 133: 33–38, 2004b.
- Perkins TA. Low power VHF transmitter for multiplexed telemetry. In: *A Handbook on Biotelemetry and Radio Tracking: Proceedings of an International Conference on Telemetry and Radio Tracking in Biology and Medicine, Oxford, 20–22 March 1979*, edited by Amlaner CJ jr and MacDonald DW. Oxford: Pergamo, 1980, p. 201–204.
- Pinkwart C and Borchers HW. Miniature three-function transmitting system for single neuron recording, wireless brain stimulation and marking. *J Neurosci Methods* 20: 341–352, 1987.
- Press WH, Teukolsky SA, Vetterling WT, and Flannery BP. *Numerical Recipes in C: the Art of Scientific Computing* (2nd ed.). Cambridge, UK: Cambridge Univ. Press, 1992.
- Reiner A, Perkel DJ, Bruce LL, Butler AB, Csillag A, Kuenzel W, Medina L, Paxinos G, Shimizu T, Striedter G, Wild M, Ball GF, Durand S, Güntürkün O, Lee DW, Mello CV, Powers A, White SA, Hough G, Kubikova L, Smulders TV, Wada K, Dugas-Ford J, Husband S, Yamamoto K, Yu J, Siang C, and Jarvis ED. Revised nomenclature for avian telencephalon and some related brainstem nuclei. *J Comp Neurol* 473: 377–414, 2004.
- Siegel JJ, Nitz D, and Bingman VP. Hippocampal theta rhythm in awake, freely moving homing pigeons. *Hippocampus* 10: 627–631, 2000.

- Siegel JJ, Nitz D, and Bingman VP.** Spatial-specificity of single-units in the hippocampal formation of freely moving homing pigeons. *Hippocampus* 15: 26–40, 2005.
- Steiner I, Bürgi C, Werffeli S, Dell’Omo G, Valenti P, Tröster G, Wolfer DP, and Lipp H-P.** A GPS logger and software for analysis of homing in pigeons and small mammals. *Physiol Behav* 71: 589–596, 2000.
- Suess E and Goiser P.** Miniaturized eight-channel telemetry system for long-term EEG registration of humans and laboratory animals. *Eur Neurol* 25, Suppl 2: 53–55, 1986.
- Takeuchi S and Shimoyama I.** A radio-telemetry system with a shape memory alloy microelectrode for neural recording of freely moving insects. *IEEE Trans Biomed Eng* 51: 133–137, 2004.
- Umbricht D, Vysotky D, Latanov A, Nitsch R, Brambilla R, D’Adamo P, and Lipp HP.** Midlatency auditory event-related potentials in mice: comparison to midlatency auditory ERPs in humans. *Brain Res* 1019: 189–200, 2004.
- Umbricht D, Vysotki D, Latanov A, Nitsch R, and Lipp HP.** Deviance-related electrophysiological activity in mice: is there mismatch negativity in mice? *Clin Neurophysiol* 116: 353–363, 2005.
- Wertz R, Maeda G, and Willey TJ.** Design for a micropowered multichannel PAM/FM biotelemetry system for brain research. *J Appl Physiol* 41: 800–805, 1976.
- Winter Y.** Construction of electronic hybrid microcircuits: a 350 mg ECG-transmitter. In: *Biotelemetry XIV*, edited by Penzel T, Salmons S, Neuman MR, Marburg: Tectum Verlag, 1998, p. 65–70.
- Yonezawa Y, Ninomiya I, and Nishiura N.** A multichannel telemetry system for recording cardiovascular neural signals. *Am J Physiol* 236: H513–518, 1979.